

High Density Polymer Brush Spontaneously Formed by the Segregation of Amphiphilic Diblock Copolymers to the Polymer/Water Interface

Manabu Inutsuka,[†] Norifumi L. Yamada,[‡] Kohzo Ito,[†] and Hideaki Yokoyama^{*,†,§}

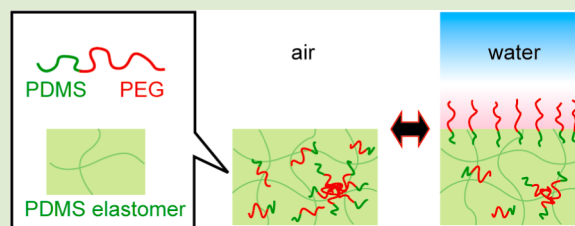
[†]Graduate School of Frontier Sciences, The University of Tokyo, Chiba 277-8561, Japan

[‡]High Energy Accelerator Research Organization, Ibaraki 319-1108, Japan

[§]Precursory Research for Embryonic Science and Technology (PRESTO), Japan Science and Technology Agency (JST), Tokyo 102-0076, Japan

Supporting Information

ABSTRACT: A self-repairable high density polymer brush of poly(ethylene glycol) (PEG) is formed at the interface between cross-linked poly(dimethyl siloxane) (PDMS) and water by spontaneous surface segregation of an amphiphilic diblock copolymer consisting of PEG and PDMS. The surface reconstruction by the formation of the brush was observed as the large hysteresis of the contact angle of the water droplet. Neutron reflectivity measurement revealed that the grafting density of the polymer brush is 2.8 chain/nm², which is comparable to those of polymer brushes by the surface-initiated polymerization method. The formation of such a remarkably dense polymer brush by segregation can be well supported by the balance between the mixing enthalpy of PEG and water and the stretching energy of PEG.



End-grafted polymer chains on surfaces are called polymer brushes and known to provide various unique properties including controls of adhesion,^{1–4} colloid stabilization,⁵ and lubrication,^{6–8} which resulted from stretched brush chains. These polymer brushes have been usually fabricated by two methods: polymerization from the surface (“grafting-from” method)⁹ or attaching a polymer chain to the surface either chemically or physically (“grafting-to” method).^{10,11} Herein we report an “inverted grafting-to” method to fabricate a hydrophilic brush layer utilizing spontaneous segregation of an amphiphilic block copolymer in a matrix of elastomer to water interface. Segregation of a block copolymer is an attractive concept for modifying interface and surface properties of polymeric materials since it requires just adding a small amount of copolymer into a homopolymer.^{12–18} In our system, copolymer can diffuse in the matrix of an elastomer even at room temperature due to the much lower glass transition temperature of the matrix. As long as the surface of the elastomer is exposed to air, the hydrophilic block buries itself in the bulk since the hydrophilic block with high surface energy avoids the air surface. However, when the surface is placed in water, the hydrophilic block starts to segregate to the surface and to form a brush layer. The copolymers segregate to cover the water interface until the chemical potentials of the bulk and brush layer are balanced; they, however, bury themselves again immediately and yield a hydrophobic elastomer surface once the surface is exposed to air or the hydrophobic environment. This polymer brush hence realizes dynamic response to environmental changes. Moreover, if some of the copolymers

at the brush layer are removed due to physical damage like frictional wear and scratch, the block copolymer chains still remaining in the bulk are supplied to the damaged surface immediately. Therefore this system potentially realizes an antifouling polymer surface with a self-repairing function that can be used for biomedical applications such as artificial vessels and organs with ever antithrombotic activity.

We constructed such a self-restoring segregation system using a cross-linked poly(dimethyl siloxane) (PDMS) elastomer for a matrix containing diblock copolymers of poly(ethylene glycol) (PEG) with the number average molecular weight (M_n) of 2100 and PDMS with M_n of 1000 (PEG–PDMS) as the amphiphilic copolymer.

The surface reconstruction behavior by the segregation of the amphiphilic copolymer was investigated by contact angle measurement of a water droplet on the sample films as shown in Figure 1. There is only a smaller difference between the advancing contact angles of PDMS containing 20 wt % of PEG–PDMS and neat PDMS. This difference is probably due to the segregation of PEG–PDMS induced by the humidity near the droplet. We confirmed that the vacuum surface before and after the contact with water is fully covered with the PDMS component by X-ray photoelectron spectroscopy (XPS) (see Supporting Information). On the other hand, the receding contact angle of PDMS with 20 wt % of PEG–PDMS is

Received: January 5, 2013

Accepted: March 5, 2013

Published: March 7, 2013

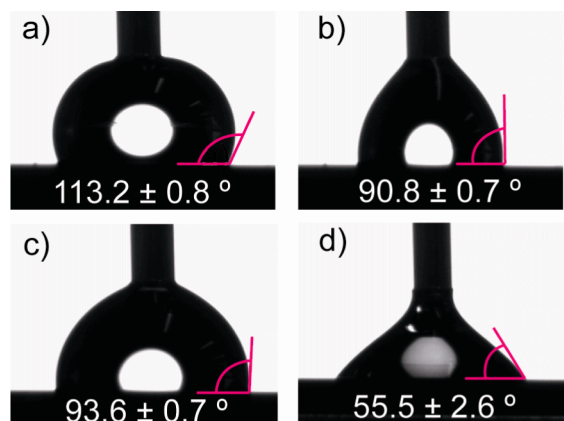


Figure 1. Images of (a) advancing and (b) receding contact angles on neat PDMS and (c) advancing and (d) receding contact angles on PDMS containing 20 wt % of PEG–PDMS. Lines in the images are a guide for the eye.

significantly smaller than that of neat PDMS. These results clearly indicate the surface reconstruction from hydrophobic to hydrophilic due to the segregation of copolymer triggered by contact with water. We did not find any dependence of contact angles on advancing and receding speed in the time scale of seconds to tens of seconds. This shows that the segregation reaches its equilibrium in seconds.

We also repeatedly observed the large hysteresis of contact angle at least several times. This fact indicates that the hydrophilic brush layer can be formed repeatedly if it once would be lost in air or a hydrophobic environment and suggests the dynamic response and the self-repairing ability of our system.

The detailed structure of the interface between PDMS films and water was investigated by neutron reflectometry. The obtained reflectivity at the interface between D₂O and PDMS containing 20 wt % of PEG–PDMS is compared to that of neat PDMS in Figure 2a. The reflectivity of neat PDMS shows only small fringes that correspond to the total thickness of the film on the quartz substrate, whereas a fringe with a larger periodicity, Δq , appeared in the reflectivity of 20 wt % PEG–PDMS, which indicates the formation of a relatively thin but well-defined D₂O-swollen polymer layer. To analyze the details of the interfacial structures, we computed the depth profiles of scattering length density (SLD) using the multilayer model mentioned in the Experimental Section. The calculated SLD profiles around the D₂O interfaces are shown in Figure 2b. A step-like layer of the mixture of polymer and D₂O can be seen on the profile of 20 wt % PEG–PDMS film irrespective of the introduction of 63 sublayers. It should be emphasized that the step-like change in SLD appeared as a result of the fit despite the 63-layer model. The thickness of the brush layer R is evaluated to be about 15 nm, corresponding to 88% of the contour length of the PEG block R_{max} ($= 17$ nm) with molecular weight of 2100. The SLD of the brush layer ρ_{brush} is $2.8 \times 10^{-4} \text{ nm}^{-2}$. This value gives the volume fraction of PEG in the brush ϕ_{PEG} , where $\phi_{\text{PEG}} = (\rho_{\text{D}_2\text{O}} - \rho_{\text{brush}})/(\rho_{\text{D}_2\text{O}} - \rho_{\text{PEG}})$, to be 0.61 and the molecular ratio in the brush layer to be 1.4 D₂O molecules per EG unit. Such a distinct layer with high volume fraction suggests the formation of a brush surface. R and ϕ_{PEG} provide the grafting density σ of the brush to be 2.8 chains/nm². Both thickness and grafting density indicate that a significantly dense brush layer is formed by the segregation of

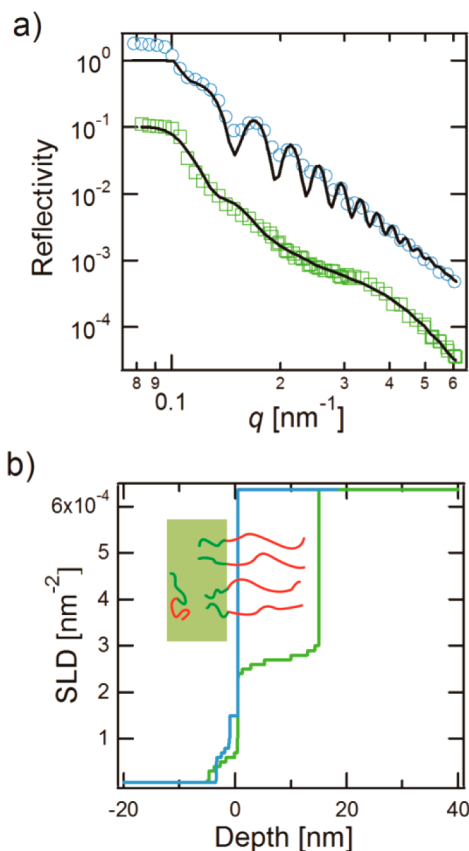


Figure 2. (a) Neutron reflectivity curves at D₂O/PDMS films containing no copolymer (blue circles) and 20 wt % of PEG–PDMS (M_n of 2100–1000, green squares) with fitting lines using multilayer models. To fit the reflectivities of 20 wt % PEG–PDMS, we needed to use the value of resolution as high as 23%, probably due to roughness of the water interface. However, such resolution does not have much of an affect on the large Δq fringes from the thin brush layer of PEG formed at the water interface. (b) The depth profiles of scattering length density around the interface of each PDMS film containing no copolymer (blue line) and 20 wt % of PEG–PDMS (green line).

the amphiphilic block copolymer. We also found that this dense brush structure was formed completely in about 8 min, and it remains at least for 2 h by neutron reflectometry (see Supporting Information). We did not find any other structure such as surface micelles or multilayer in this time range.

The formation of such a highly dense and extremely stretched brush layer by segregation is surprising because it encounters unfavorable stretch and hence loss of configurational entropy in the PEG block. In our system, the main driving force for the formation of the brush layer is hydration energy of PEG blocks. If this is sufficiently larger than the stretching energy of the brush chains, such a dense and stretched polymer brush is possible. The most significant difference between the conventional polymer brush by “grafting-to” or “grafting-from” methods and ours is whether the grafting density σ is fixed or variable. When a conventional brush chain with fixed σ is placed in water, it will be swollen, and the volume fraction of polymer in the brush layer decreases until the hydration saturates. More swelling never happens because it gives only stretching entropic loss. On the other hand, our brush by segregation of copolymer can optimize both elongation R/R_{max} and σ . The brush chains can be denser to

maximize the hydration energy gain per unit area at the cost of stretching energy. Therefore, conventional brushes with fixed σ reach only a local minimum, whereas brush by segregation can scan the global minimum in the energy map of R/R_{\max} and σ .

To verify this idea, we have calculated free energy per unit area by the formation of brush layer F as a function of R/R_{\max} and σ . Some models have already reported the structures of swollen polymer brushes^{19,20} and block copolymers at the interface between polymers.^{21,22} In this report, however, we consider only the balance between the hydration energy of the PEG block and the stretching energy of both PEG and PDMS. For the evaluation of hydration energy per chain F_{int} , we used interaction energy ΔU of the PEG 2000–water system experimentally obtained using an ultrasonic technique by Faraone et al.²³ To evaluate the stretching energy F_{ent} , we assume that the stretching of the chain under the applied force f is described by the Langevin function²⁴

$$\frac{R}{R_{\max}} = L\left(\frac{fb}{k_{\text{B}}T}\right) = \coth\left(\frac{fb}{k_{\text{B}}T}\right) - \left(\frac{fb}{k_{\text{B}}T}\right)^{-1} \quad (1)$$

where k_{B} is the Boltzmann constant; T is temperature; and b is the Kuhn monomer length. Integrating the inverse function of eq 1 yields the stretching energy

$$F_{\text{ent}} = k_{\text{B}}TN \left[\frac{R}{R_{\max}} L^{-1}\left(\frac{R}{R_{\max}}\right) - \ln\left\{ \sinh L^{-1}\left(\frac{R}{R_{\max}}\right) \right\} + \ln\left\{ L^{-1}\left(\frac{R}{R_{\max}}\right) \right\} \right] \quad (2)$$

where N is the number of Kuhn monomers of the chain. Molar masses of Kuhn monomers of PEG block and PDMS block are 137 and 381, respectively.²⁴ Let us evaluate the stretching energy of the PDMS anchor block. Neutron reflectivity provides no information on the conformation of the anchor PDMS block, but we assume that the elongation of the PDMS chain is the same as that of the PEG brush chain. Actually, the stretching energy of the PDMS block is negligibly smaller than that of PEG because the number of Kuhn monomers of PDMS is only 2.6, which is much smaller than that of PEG of 15.3.

After all, F is written as the sum of hydration and stretching energies

$$F = \sigma[F_{\text{int}} + F_{\text{ent}}] \quad (3)$$

Figure 3 shows the calculated F as a function of R/R_{\max} and σ at 293 K. This map qualitatively supports that the brushes with fixed σ reach only a local minimum, whereas brush by segregation can be more stretched and denser to reach the global minimum. Actually, our brush is more stretched and denser than the prediction of the model ($R/R_{\max} = 0.72$ and $\sigma = 1.8$ chains/nm²). This is probably because F_{int} is underestimated: the PEG block gains energy not only by mixing enthalpy of PEG and water but also by reducing unfavorable contact of PEG and PDMS via forming the brush layer.

In our model, the driving force of the segregation is the enthalpic gain by solvation of the brush block. Therefore, such a dense brush structure can only be formed with the particular combination of polymers and solvents which give a large solvation energy gain. The combination of water and PEG shows a unique hydration behavior as reported in previous reports.^{25,26}

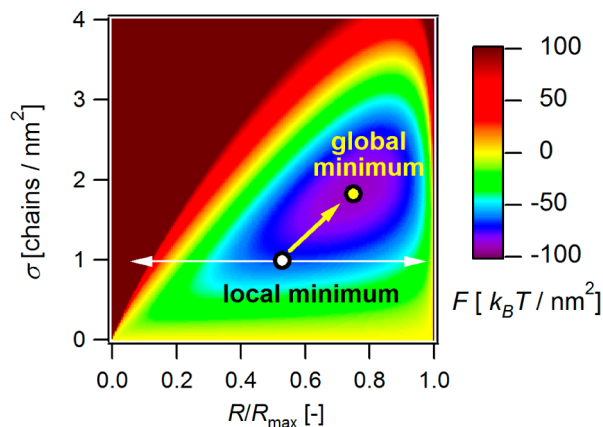


Figure 3. Calculated free energy change by hydration and stretching of the PEG brush as a function of elongation R/R_{\max} and grafting density σ . Circles and arrays on the figure schematically show the difference between conventional brush and brush by segregation. Conventional brushes can search only in the R/R_{\max} direction to find the local minimum in swelling, while brush by segregation can also vary σ to reach the global minimum.

In summary, we have succeeded in preparing the high density and extremely stretched PEG polymer brush by a spontaneous segregation process. The free energy calculation proved that these remarkable results are due to the two characteristics of brush by segregation. First, the formation of our brush is driven by hydration energy gain of PEG. Second, our brush can optimize both the elongation and grafting density to reach the global minimum.

EXPERIMENTAL SECTION

Film Preparation. PEG–PDMS with M_n of 2100 for the PEG block and 1000 for the PDMS block (Polymersource, Inc.; based on the information by the supplier, polydisperse indexes of each block are 1.02 for PEG and 1.2 for PDMS), vinyl terminated PDMS with molecular weight of $\sim 25\,000$ (PDMS-V, Aldrich, Inc.), and poly(methylhydrosiloxane-co-dimethylsiloxane) with molecular weight of ~ 950 (50–55% of dimethylsiloxane, PHDMS, Aldrich, Inc.) were dissolved in dehydrated tetrahydrofuran (THF, Wako Pure Chemical Industries, Ltd.). The ratios of PDMS-V to PHDMS and PEG–PDMS to (PDMS-V + PHDMS) were 9 to 1 and 2 to 8, respectively. The resulting block copolymer fraction was 20 wt %, and the total polymer concentration in THF was 2.5 wt %. The platinum–1,3-divinyl-1,1,3,3-tetramethylsiloxane complex in xylene (Aldrich, Inc., $\sim 2\%$ platinum) was added to the polymer solution as catalyst for cross-linking, and then immediately the solution was spin-coated at 2000 rpm onto silicon or thick quartz wafers. The cross-linking reaction of homo-PDMS occurs in part during evaporation of the solvent. These films were further annealed at 70 °C for 6 h in vacuo for the remaining functional groups of PDMS to be fully cross-linked. The thicknesses of the PDMS films on silicon substrates were in the range of 160–180 nm, which were estimated by ellipsometry (JASCO, M-150).

XPS Measurement. The surface analysis in vacuum was investigated by XPS (ULVAC-PHI, Inc., Quantum 2000) using Al K α .

Contact Angle Measurement. Surface reconstruction by the segregation of PED–PDMS was observed by contact angle measurement (dataphysics, OCA 15 plus) of a water droplet on sample films. A droplet of distilled water (5 μL) was placed onto the sample film and then expanded and shrunk by 10 μL at 0.1–2.0 $\mu\text{L}/\text{s}$ via a needle from a syringe. Images of the droplets were captured by a CCD camera and analyzed to obtain the advancing and receding contact angles.

Neutron Reflectivity Measurement. Neutron reflectometry experiments were conducted with Advanced Reflectometer for Interface and Surface Analysis II (ARISA-II)²⁷ and Soft Interface Analyzer (SOFIA)^{28,29} at J-PARC. Specular neutron reflectivity of the

interface between the polymer and D₂O was measured more than 1 h after the contact with water. The depth profiles of SLD were computed by fitting the reflectivity curves using Parratt32 (version 1.6, developed by C. Braun at the Hahn-Meitner-institut Berlin). We fitted the reflectivity curves with a multilayer model consisting of quartz substrate, PDMS matrix film, D₂O-swollen brush layer, and D₂O ambient. The SLDs of quartz, the PDMS matrix, PEG, and D₂O were assumed to be 4.2, 0.06, 0.56, and $6.36 \times 10^{-4} \text{ nm}^{-2}$, respectively. The brush layer was divided into 63 sublayers whose SLDs were fixed at 0.1, 0.2, ..., $6.3 \times 10^{-4} \text{ nm}^{-2}$ with 0.1 increments, and the thickness of each layer was used as fitting variables. Employing this fitting method automatically assumes monotonic decrease of the volume fraction of PEG ϕ_{PEG} along the distance from matrix surface z . The thicknesses of 63 sublayers as fitting parameters were optimized to obtain the SLD profiles around the sample film/D₂O interfaces.

■ ASSOCIATED CONTENT

■ Supporting Information

XPS data, time-division neutron reflectivity, and details of free energy calculations. This material is available free of charge via the Internet at <http://pubs.acs.org>.

■ AUTHOR INFORMATION

Corresponding Author

*E-mail: yokoyama@molle.k.u-tokyo.ac.jp.

Notes

The authors declare no competing financial interest.

■ ACKNOWLEDGMENTS

This work has been financially supported by PRESTO-JST. The neutron reflectometry experiments were performed using SOFIA and ARISA II at J-PARC with the support from the S-type research project of KEK (2009S08). The XPS experiments were performed using Quantan 2000 (ULVAC PHI, Inc.) at AIST.

■ REFERENCES

- (1) Jeon, S. I.; Lee, J. H.; Andrade, J. D.; De Gennes, P. G. *J. Colloid Interface Sci.* **1991**, *142*, 149–158.
- (2) Amaji, M.; Park, K. *J. Biomater. Sci., Polym. Ed.* **1993**, *4*, 217–234.
- (3) Halperin, A. *Langmuir* **1999**, *15*, 2525–2533.
- (4) Leckband, D.; Sheth, S.; Halperin, A. *J. Biomater. Sci., Polym. Ed.* **1999**, *10*, 1125–1147.
- (5) Vincent, B. *Adv. Colloid Interface Sci.* **1974**, *4*, 193–277.
- (6) Klein, J. *Annu. Rev. Mater. Sci.* **1996**, *26*, 581–612.
- (7) Joanny, J.-F. *Langmuir* **1992**, *8*, 989–995.
- (8) Kobayashi, M.; Terayama, Y.; Hosaka, N.; Kaido, M.; Suzuki, A.; Yamada, N.; Torikai, N.; Ishihara, K.; Takahara, A. *Soft Matter* **2007**, *3*, 740–746.
- (9) Tsujii, Y.; Ohhno, K.; Yamamoto, S.; Goto, A.; Fukuda, T. *Adv. Polym. Sci.* **2006**, *197*, 1–45.
- (10) Halperin, A.; Tirrell, M.; Lodge, T. P. *Adv. Polym. Sci.* **1992**, *100*, 31–71.
- (11) Zhao, B.; Brittain, W. J. *Prog. Polym. Sci.* **2000**, *25*, 677–710.
- (12) Shull, K. R.; Kramer, E. J.; Hadziioannou, G.; Tang, W. *Macromolecules* **1990**, *23*, 4780–4787.
- (13) Green, P. F.; Russell, T. P. *Macromolecules* **1991**, *24*, 2931–2935.
- (14) Dai, K. H.; Kramer, E. J.; Shull, K. R. *Macromolecules* **1992**, *25*, 220–225.
- (15) Kassis, C. M.; Steehler, J. K.; Betts, D. E.; Guan, Z.; Romack, T. J.; DeSimone, J. M.; Lonton, R. W. *Macromolecules* **1996**, *29*, 3247–3254.
- (16) Iyengar, D. R.; Perutz, S. M.; Dai, C. -A.; Ober, C. K.; Kramer, E. J. *Macromolecules* **1996**, *29*, 1229–1234.

- (17) Mansky, P.; Russell, T. P.; Hawker, C. J.; Mays, J.; Cook, D. C.; Satija, S. K. *Phys. Rev. Lett.* **1997**, *79*, 237–240.
- (18) Yokoyama, H.; Miyamae, T.; Han, S.; Ishizone, T.; Tanaka, K.; Takahara, A.; Torikai, N. *Macromolecules* **2005**, *38*, 5180–5189.
- (19) Alexander, S. *J. Phys. (Paris)* **1977**, *38*, 977–981.
- (20) Minler, S. T.; Witten, T. A.; Cates, M. E. *Macromolecules* **1988**, *21*, 2610–2619.
- (21) Leibler, L. *Makromol. Chem., Macromol. Symp.* **1988**, *16*, 1–17.
- (22) Shull, K. R.; Kramer, E. J. *Macromolecules* **1990**, *23*, 4769–4779.
- (23) Faraone, A.; Magazù, S.; Maisano, G.; Migliardo, P.; Tettamanti, E.; Villari, V. *J. Chem. Phys.* **1999**, *110*, 1801–1806.
- (24) Rubinstein, M.; Colby, R. H. *Polymer Physics*; Oxford University Press: New York, 2003.
- (25) Graham, N. B.; Zulfiqar, M.; Nwachuku, N. E.; Rashid, A. *Polymer* **1988**, *30*, 528–533.
- (26) Lüsse, S.; Arnold, K. *Macromolecules* **1996**, *29*, 4251–4257.
- (27) Mitamura, K.; Yamada, N. L.; Sagehashi, H.; Seto, H.; Torikai, N.; Sugita, T.; Furusaka, M.; Takahara, A. *J. Phys. Conf. Ser.* **2011**, *272*, 012017.
- (28) Yamada, N. L.; Torikai, N.; Mitamura, K.; Sagehashi, H.; Sato, S.; Seto, H.; Sugita, T.; Goko, S.; Furusaka, M.; Oda, T.; Hino, M.; Fujiwara, T.; Takahashi, H.; Takahara, A. *Eur. Phys. J. Plus* **2011**, *126*, 108.
- (29) Mitamura, K.; Yamada, N. L.; Sagehashi, H.; Torikai, N.; Arita, H.; Terada, M.; Kobayashi, M.; Sato, S.; Seto, H.; Gokou, S.; Furusaka, M.; Oda, T.; Hino, M.; Jinnai, H.; Takahara, A. *Polym. J.* **2013**, *45*, 100–108.